Self-aggregation behaviour of novel thiosemicarbazone drug candidates with potential antiviral activity†

Romina J. Glisoni,[abc] Diego A. Chiappetta,[ac] Liliana M. Finkielsztein,[b] Albertina G. Moglioni[bc] and Alejandro Sosnik*[ac]

The present work aimed to gain further insight into the mechanisms governing the aggregation process of 1-indanone thiosemicarbazone drug candidates. Regardless of the relatively low lipophilicity predicted by theoretical calculations, these compounds were very insoluble in water. This performance was especially notorious for methoxylated (and non-N-allylated) derivatives. Thermal analysis revealed that the introduction of one and two $CH_3O–$ moieties into the aromatic ring increases the T_m pronouncedly from 185 °C to 229 °C and 258 °C, respectively. The formation of nano-aggregates in water was suggested by the appearance of a new strong absorption peak at 233–239 nm in the UV spectra. DLS analysis showed the early formation nanoscopic particles (120–300 nm) that undergo a gradual size growth to generate larger submicron structures; these particles remained invisible to the naked eye. The negatively-charged character of the surface was established by zeta potential measurements. These results suggest the generation of an inner hydrophobic "core" due to the interaction of highly hydrophobic aromatic rings that is surface-decorated by C=S groups available in a thiolato anionic form. This aggregation mechanism is supported by the fact that methoxylation of the aromatic ring dramatically strengthens the solute–solute affinity, as expressed by the sharp increase in T_m and makes these derivatives much more water-insoluble. Finally, overall findings indicate that for these compounds, solubility predictions based on lipophilicity calculations are not reliable and a more thorough characterization is required.

1. Introduction

Since Domagk et al. described the activity of thiosemicarbazones (TSCs) against experimental tuberculosis,[1,2] the antineoplastic,[3] antibacterial,[4] antifungal,[5] antiprotozoal[6] and antiviral[7–9] activity of a great number of TSCs has been extensively investigated. Some of these derivatives displayed tuberculostatic activity in concentrations > 20 μg ml^{-1}.[10,11] In some cases, the pharmacological activity is conferred by a metallic ion (e.g., iron) associated with the TSC molecule to form a complex.[12] Regardless of the therapeutic potential investigated for over six decades, only a few TSC drug candidates have been approved by the US FDA and implemented in clinics,[13] namely the oral antiseptic ambazone[14] and the antiviral methisazone.[15] The antitumoral activity of

3-aminopyridine-2-carboxaldehyde thiosemicarbazone[16] is being currently evaluated in Phase I and II clinical trials for the treatment of various metastatic and solid cancers.[13,17] It has been demonstrated that heterocyclic TSCs act by inhibiting the ribonucleotide reductase, an enzyme involved in the biosynthesis of DNA precursors.[18]

Moglioni et al. have designed, synthesized and characterized different TSC derivatives of aromatic and aliphatic ketones.[19–21] The activity of these novel compounds is being currently investigated in vitro against different pathogens: (i) the Junin virus (JUNV), the causative agent of the Argentine Hemorrhagic Fever (AHF),[22] (ii) Gram negative and positive bacteria and fungi,[21] (iii) Trypanozoma cruzi, the causative agent of Chagas disease and (iv) the virus of the bovine viral diarrhea (BVDV);[23] BVDV is a surrogate model of the Hepatitis C virus (HCV), which is difficult to culture and replicate under in vitro conditions.[24]

Remarkably, 5,6-dimethoxy-1-indanone TSC has shown a 7-fold increase in the selectivity index (SI = 80.29) against BVDV with respect to ribavirin (SI = 11.64);[23] ribavirin is the first-choice drug used in the anti-HCV pharmacotherapy combined with pegylated interferon alpha.[25] These promising preliminary results have motivated us to investigate systematically the antiviral activity of a series of 1-indanone TSCs with different patterns of substitution in both the aromatic ring and the terminal –NH₂ group.

TSCs are extremely poorly water soluble.[21–23] To evaluate the activity of 1-indanone TSCs in vitro, the drug candidate is
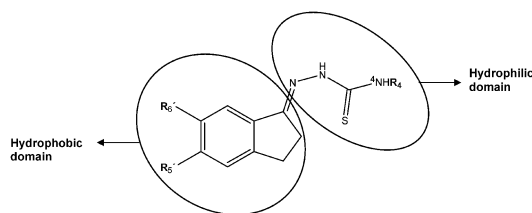
[a] The Group of Biomaterials and Nanotechnology for Improved Medicines (BIONIMED), Department of Pharmaceutical Technology, Faculty of Pharmacy and Biochemistry, University of Buenos Aires, 956 Junín St., 6th Floor, Buenos Aires CP1113, Argentina. E-mail: alesosnik@gmail.com; Fax: ; Tel: +54-11-4964-8273
[b] Department of Pharmacology, Faculty of Pharmacy and Biochemistry, University of Buenos Aires, Buenos Aires CP1113, Argentina
[c] National Science Research Council (CONICET), Buenos Aires, Argentina

Table 1 Chemical structure, HR-MS, UV and T_m data of the different TSCs. The hydrophobic and the hydrophilic domains in the molecule are pointed out

TSC	Substituents	MW^a (m/z) [M + H$^+$]	DMSO	Water:DMSO	$\varepsilon^d/10^4$ M^{-1}cm^{-1}	$T_m^e/$°C
				λ/nm		
1-indanone thiosemicarbazone	$R_{4,5',6'}$ = H	206.0746	332 320^b 294 283	324 312^b 290 280 233^c	2.73	185
6-methoxy-1-indanone thiosemicarbazone	$R_{4,5'}$ = H, $R_{6'}$ = OCH$_3$	236.0852	345 330^b 306 295	337 324^b 299 289 233^c	2.81	229
5,6-dimethoxy-1-indanone thiosemicarbazone	R_4 = H, $R_{5',6'}$ = OCH$_3$	266.0957	348 334^b 299 288	343 329^b 293 283 233^c	3.47	258
5,6-dimethoxy-1-indanone N4-allylthiosemicarbazone	$R_{5',6'}$ = OCH$_3$, R_4 = CH$_2$CH=CH$_2$	306.1270	352 336^b 299 288	345 330^b 294 284 239^c	4.00	199

^{a} Molecular weight obtained by High Resolution-Mass Spectrometry (HR-MS). ^{b} λ_{max} used in solubility, physical stability, and HPLC assays. ^{c} New λ in water–DMSO (98 : 2) solutions that appears at day 0 and increases over time. ^{d} Molar extinction coefficients (ε) in DMSO. ^{e} T_m determined by DSC.

primarily solubilized in dimethyl sulfoxide (DMSO) and then diluted in culture medium to the final TSC concentration of study.[23] The maximum TSC concentration attainable in solution is often limited by the DMSO cytotoxicity that ranges between 0.5% and 2.0% v/v. Also, these derivatives precipitate very rapidly during the *in vitro* assays, leading to erratic, non-reproducible and unreliable antiviral half maximal inhibitory concentration (IC$_{50}$) data.[26] Thus, the extremely low aqueous solubility found for these and other TSCs[27–29] remains a key hurdle towards their biological evaluation.

Lipophilicity is the measure of the degree to which a molecule prefers a non-polar over an aqueous environment and it is estimated by the logarithm of the octanol–water partition coefficient (log P). Log P is one of the parameters considered in the "Lipinski Rule of 5" to determine the pharmacokinetic properties expected for a specific molecule.[30] Theoretical values can be calculated by means of the fragmentation approach;[31] *e.g.*, unsubstituted 1-indanone TSC displays a theoretical log P of approximately 0.4. However, this value is not consistent with the extremely low experimental solubility observed in water.

The self-aggregation in aqueous solution of penicillins (*e.g.*, cloxacillin),[32,33] antidepressants (*e.g.*, imipramine),[34] antipsychotics (*e.g.*, trifluoperazine dihydrochloride)[35] and polyene antibiotics (*e.g.*, amphotericin B)[36] has been previously reported. Nano-aggregates have been characterized by (i) light scattering analysis[32,37,38] and (ii) the appearance of new absorption peaks in the UV.[39,40]

1-Indanone TSC molecules combine a bulky hydrophobic aromatic ring and a highly hydrophilic thiosemicarbazone

group (Table 1). This structure confers the molecule an amphiphilic character and might account for their aggregation in water.

The present work investigated for the first time the mechanisms governing the self-aggregation of TSCs in water. Overall data indicate the fast initial formation of negatively-charged nano-aggregates that gradually grow in size to generate larger clusters, these structures serving as nuclei for the later crystallization and precipitation of the compound in water.

2. Materials and methods

2.1 Materials

Different TSC derivatives were synthesized by the reaction between 1-indanone, 6-methoxy-1-indanone and 5,6-dimethoxy-1-indanone (Sigma-Aldrich, St. Louis, MO, USA) and thiosemicarbazide or N4-allylthiosemicarbazide (Sigma-Aldrich), as described elsewhere.[23] The synthesis and characterization of 5,6-dimethoxy-1-indanone N4-allylthiosemicarbazone is described here for the first time. Briefly, 5,6-dimethoxy-1-indanone (1.00 g, 5.20 mmol) and N4-allylthiosemicarbazide (1.10 g, 8.38 mmol) were dissolved in hot water–ethanol (1 : 1) and magnetically stirred until total dissolution. Glacial acetic acid (0.25–0.30 ml) was added and the reaction mixture was refluxed overnight. Then, the solution was cooled to 4 °C and stored overnight in the refrigerator. The white precipitate was collected by vacuum filtration, washed with cold water–ethanol (1 : 1) and recrystallized (see below). The yield of the reaction was 80%. To assure the high purity of all the TSCs used in the

study, samples (1 g) were solubilized in cold DMSO (100 ml) and poured into ultra-pure water (500 ml). Precipitates were isolated by filtration, thoroughly washed with ultra-pure water to remove DMSO residues and dried at room temperature until constant weight. Before this purification step, TSCs showed traces of the corresponding 1-indanone derivative in ^{1}H-NMR spectra.

The Fourier transform infrared (FT-IR) spectrum of 5,6-dimethoxy-1-indanone N4-allylthiosemicarbazone was recorded in a Perkin-Elmer One FT-IR spectrophotometer (KBr pastilles, Waltham, MA, USA). Characteristic thiosemicarbazone bands were found at (cm^{-1}): 3354.9 ν (NH st); 3205.9 ν (NH st); 1604.3 ν (C=N st); 1527.2 ν {C(S)–N st}; 1490.9 ν (C=S st). Allyl group bands were found at (cm^{-1}): 1644.5, 958.4 and 922.5 ν (CH$_2$–CH=CH$_2$ st).
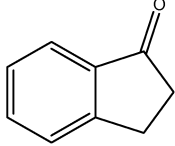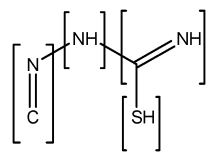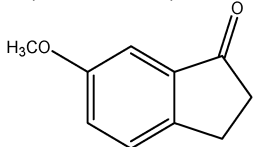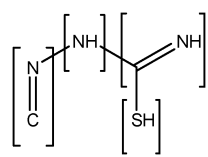
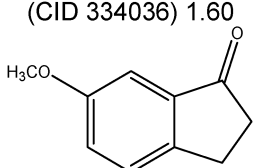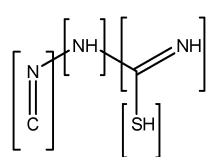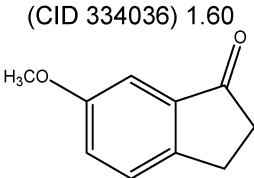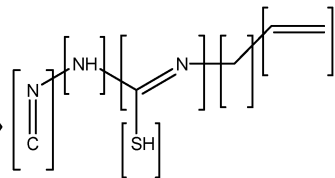The experimental molecular weight (*m/z*) of the different TSCs was determined by high resolution mass spectrometry (HR-MS, micrOTOF-Q II, Bruker Daltonics, Germany) using electrospray ionization (ESI) as the ionization source type. Data are summarized in Table 1.

Proton nuclear magnetic resonance (^{1}H-NMR) spectra were obtained from deuterated DMSO (DMSO-d_6, Sigma) solutions at room temperature on a Bruker MSL300 spectrometer (Karlsruhe, Germany), at 300 MHz. The spectrum of the N4-allyl derivative was similar to that of 5,6-dimethoxy-1-indanone thiosemicarbazone (Fig. S1A, ESI†), though it displayed the protons corresponding to the allyl group and the partition of the signal belonging to the terminal –NH– group (Fig. S1B†).

Carbon nuclear magnetic resonance (^{13}C-NMR) analysis of the N4-allyl derivative was carried out in a Varian Mercury-200 NMR spectrometer (DMSO-d_6 solution, 25 °C, Oxford, UK). δ were found at (ppm): 178.2; 158.3; 152.6; 149.4; 142.9; 136.1; 130.2; 116.1; 108.5; 104.7; 56.5; 56.3; 46.4; 28.7; 28.4. The specific signals of the allyl group were found at (ppm): 136.1 (CH$_2$–CH=CH$_2$), 116.1 (CH$_2$–CH=CH$_2$) and 46.4 (*C*H$_2$–CH=CH$_2$).

Table 1 summarizes the molecular properties of the four TSCs considered in the present study. The solvents used were of analytical grade and were used as received.

Table 2 log k_w, log P values and fragmentation approach for the calculation of log P by the Fujita-Hansch method

TSC	log $k_w{}^a$	log $P_a{}^b$	log $P_b{}^c$	Pubchem Base log P	Hansch-Fujita π substituent constants	log $P_c{}^d$
1-Indanone thiosemicarbazone	1.95	1.79	1.49	(CID 6735) 1.70		log P = [(1.70; 1-indanone) − (−1.21; C=O)] + [(−0.84 × 2; C=N–) + (−1.19; –NH–) + (0.39; –SH)] = 0.43
6-methoxy-1-indanone thiosemicarbazone	2.03	1.66	1.36	(CID 334036) 1.60		log P = [(1.60; 6-methoxy-1-indanone) − (−1.21; C=O)] + [(−0.84 × 2; C=N–) + (−1.19; –NH–) + (0.39;–SH)] = 0.33
5,6-dimethoxy-1-indanone thiosemicarbazone	1.79	1.54	1.24	(CID 334036) 1.60		log P = [(1.60; 6-methoxy-1-indanone) – (0; Ar–H) + (−0.02; Ar–OCH$_3$) − (−1.21; C=O)] + [(−0.84 × 2; C=N–) + (−1.19; –NH–) + (0.39; –SH)] = 0.31
5,6-dimethoxy-1-indanone N4-allyl thiosemicarbazone	2.83	2.75	2.59	(CID 334036) 1.60		log P = [(1.60; 6-methoxy-1-indanone) – (0; Ar–H) + (−0.02; Ar–OCH$_3$) − (−1.21; C=O)] + [(−0.84 × 2; C=N–) + (−1.19; –NH–) + (0.39; –SH) + (0.50; –CH$_2$) + (0.70; CH=CH$_2$)] = 1.51

^{a} Log k_w calculated by RP-HPLC. ^{b} Log P_a calculated by Spartan '02 software (Ghose-Crippen method). ^{c} Log P_b calculated by Chemdraw Ultra 7.0 software. ^{d} Log P_c calculated by the Fujita-Hansch method. Values for each substituent were extracted from ref. 37 and 38.

2.2 Determination of the theoretical lipophilicity

The theoretical logarithms of partition coefficients (log P) were calculated by means of the fragmentation approach based on the sum of Hansch-Fujita π constants;[31,41,42] this parameter describes the contribution of each substituent to the lipophilicity of a compound. The fragmentation approach used for these calculations is summarized in Table 2. Basic log P values for 1-indanone and 6-methoxy-1-indanone were obtained from Pubchem (National Center for Biotechnology Information, Bethesda, MD, USA). Complementary computational calculations were performed by means of ChemDraw Ultra 7.0 (CambridgeSoft, Cambridge, MA, USA) and Spartan '02 (Ghose-Crippen method, Wavefunction Inc, Irvine, CA, USA) softwares.

2.3 Determination of the experimental lipophilicity

Experimental logarithms of capacity factor (log k) were calculated by liquid chromatography (HPLC, Waters 590 HPLC Pump) with an ultraviolet detector (320–336 nm, Jasco-975, Software WinPcChrom XY, Jasco Inc, Easton, MD, USA) and a Sunfire™ column C18, 5.0 μm, 4.6 × 150 mm (Waters Corp., Milford, MA, USA). Stock solutions of each TSC in DMSO (3.5 μg ml^{-1}) were injected (10 μl) and a mobile phase composed of acetonitrile–buffer phosphate pH 7.0 (29 mM) of different volume ratios (20 : 80, 25 : 75, 30 : 70, 40 : 60, 45 : 55, 50 : 50 and 55 : 45) was pumped at a flow rate of 1.0 ml min^{-1}.[43,44] Logarithms of capacity factor (log k) were calculated as follows:

$$\log k = \log[(t_r - t_o)/t_o]$$

t_r an t_o being the retention time and the dead time (solvent front, DMSO), respectively.

A curve of log k versus the percentage of acetonitrile (%) in the mobile phase was built and log k_{water} (log k_w) values were extrapolated at 0% acetonitrile. Experimental values were compared to those obtained by theoretical and computational calculations.[45] To correlate computational and experimental data, log P versus log k_w curves were built.

2.4 Solubility studies

The solubility of the different TSCs in pure DMSO and water–DMSO (98 : 2) was studied by UV spectrophotometry; 2% DMSO is the maximum concentration usually tolerated by cell monolayers in vitro. A 75 μM stock solution was prepared and subsequently diluted to obtain 7.5, 15.0, 22.6 and 37.5 μM solutions. The absorbance was measured at the corresponding λ_{max} established for each TSC (CARY [1E] UV–Visible Spectrophotometer Varian, Palo Alto, CA, USA) at 23 °C. Molar extinction coefficients (ε) were calculated according to the Lambert–Beer law from absorbance versus concentration plots (Table 1). Concentrations were calculated by interpolating the absorbance of each sample in a calibration curve covering the range between 7.5 and 75 μM (correlation factors were 0.9923–1.0000), that was built for each compound. Solvents were used as blank. Experiments were carried out in duplicate and concentrations are expressed in μM. The intrinsic solubility (S_o) of each TSC in aqueous medium was defined as the highest concentration measured for any of the solutions at day 30. To estimate the aggregation tendency, the ratio between the intensity of a new peak found in water–DMSO at 233 nm (239 nm for the N4-allyl derivative) and that of the λ_{max} ($I_{233}/I_{\lambda_{max}}$) was calculated, at day 30; the sample used for this calculation was the same of S_o.

2.5 Thermal analysis

To measure the melting temperature (T_m) of the different derivatives, TSCs (5–7 mg) were sealed in 40 μl Al-crucible pans and analyzed by Differential Scanning Calorimetry (DSC, Mettler TA-400 differential scanning calorimeter) in a single heating ramp (25–350 °C, 10 °C min^{-1}).

2.6 Dymanic light scattering (DLS)

The aggregation parameters (size, intensity size distribution and zeta potential) of TSCs aggregates (7.5–75 μM) in water–DMSO (98 : 2) were studied by Dynamic Light Scattering (DLS, Zetasizer Nano-Zs, Malvern Instruments, UK) provided with a 4 mW He–Ne (633 nm) laser and a digital correlator ZEN3600, at 25 °C, scattering angle of 173°, and 4.65 mm measurement position. Samples were prepared as previously described (see UV experiments), and filtered by clarifying filters (0.45 μm, cellulose nitrate) prior to the analysis. Refractive indexes for each sample (RI = 1.3344–1.3354) were measured in a Refractometer Officine Galileo N°51986 (Italy), at 25 °C. Results are expressed as the average of four measurements. Data were analyzed using CONTIN algorithms (Malvern Instruments). The polydispersity index (PDI) was also determined; PDI is a measure of the size distribution and the homogeneity of the sample. To evaluate the physical stability of the dispersions, TSCs samples were incubated at 25 °C and the same parameters monitored over 1 month.

2.7 Microscopy

The morphology of the aggregates of 5,6-dimethoxy-1-indanone TSC (7.5 μM) at days 0 and 30 was studied by means of transmission electron microscopy (TEM, Philips CM-12 TEM apparatus, FEI Company, Eindhoven, The Netherlands). Samples (5 μl) were placed onto a grid covered with Fomvar film. After 30 s, the excess was carefully removed with filter paper and phosphotungstic acid (2% w/v, 5 μl) was added. After 30 s, the excess was removed and water (5 μl) was added and left for 30 s and removed. Samples were finally dried in a closed container with silicagel and analyzed. The diameter of the nanoparticles was estimated using a calibrated scale. A more concentrated system (150 μM) of the same TSC was also visualized by optical microscopy (Arcano XSZ-107 E, Argentina).

2.8 Surface tension measurements

The surface tension of TSC solutions ranging between 7.5 and 75 μM was measured by means of the du Noüy ring method (Fernández Berlusconi y Rocca SRL, Argentina), at 23 °C ± 0.5 °C.

3. Results and discussion

3.1 Lipophilicity

Despite their potential therapeutic activity against a broad spectrum of pathogens, only a few TSCs have reached the clinical stages. A main technological drawback towards their preliminary biological evaluation and activity screening is the extremely low aqueous solubility of most of these derivatives, this phenomenon being especially remarkable when the TSC is derived from an aromatic ketone.[46,47] In this context, two main issues of concern are emerging. First, the intrinsic aqueous solubility of new TSC candidates is often unknown; compounds are generally referred as "poorly water soluble" though no quantitative determinations are conducted.[47] Moreover, IC_{50} studies not always consider that these molecules might aggregate in aqueous media and form from nano to submicron-particles that are invisible to the naked eye and remain in suspension. The latter might result in effective concentrations in solution that are lower than those *a priori* calculated; we have observed the gradual precipitation of TSCs in different culture media during *in vitro* assays and also in stock solutions of these new drug candidates.[26] Surprisingly, despite the impact that this phenomenon might have on the biological results, it was not previously investigated.

A first indication that the behaviour of 1-indanone TSC derivatives in water deviates from the predicted one is the gap found between theoretical log *P* values and computational and experimental determinations (log k_w) (Table 2). According to calculations, the incorporation of one $CH_3O–$ functional group into the unsubstituted aromatic ring makes the TSC more hydrophilic, owing to the ability of the O atom to form H bonds; log *P* determined by means of Hansch-Fujita decreases from 0.43 for 1-indanone TSC to 0.33 and 0.31 for mono and dimethoxy derivatives, respectively. The fragmentation approach is shown in Table 2. As expected, the substitution of the terminal –NH_2 with a hydrophobic allyl group generated a significantly more lipophilic molecule (log *P* = 1.51). Computational methods predicted more hydrophobic structures (Table 2); log *P* values ranged between 1.24–1.54 and 2.59–2.75 for 5,6-dimethoxy-1-indanone TSC and the N4-allyl derivative, respectively. log k_w values determined by HPLC indicated that 1-indanone TSCs are more hydrophobic than the theoretical predictions (Fig. 1). For example, 1-indanone and 5,6-dimethoxy-1-indanone TSCs showed log k_w values of 1.95 and 1.79. In any advent, all these approaches indicated that 5,6-dimethoxy-1-indanone is more hydrophilic than the unsubstituted one. Conversely, the 6-methoxy derivative is slightly more hydrophobic than the unsubstituted molecule, the log k_w being 2.03. The good correlation between the experimental data and both computational methods is shown in Fig. 2.

Based on lipophilicity determinations, dimethoxylated TSCs are expected to show better aqueous solubility than 1-indanone-TSC. On the other hand, the contribution of one methoxyl group to the hydrophilicity of the molecule appears as less crucial.
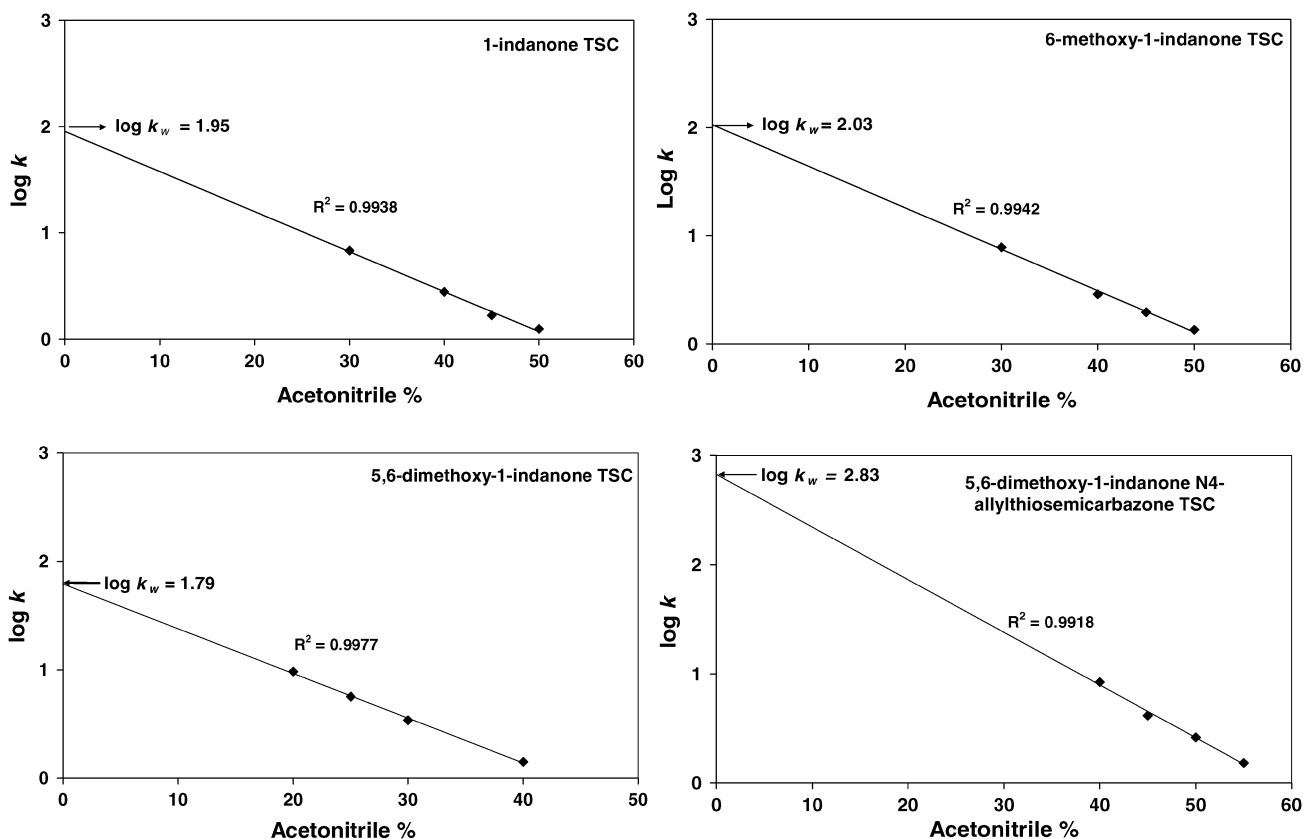

Fig. 1 Experimental lipophilicity (log k_w) of the different 1-indanone TSCs as determined by HPLC.
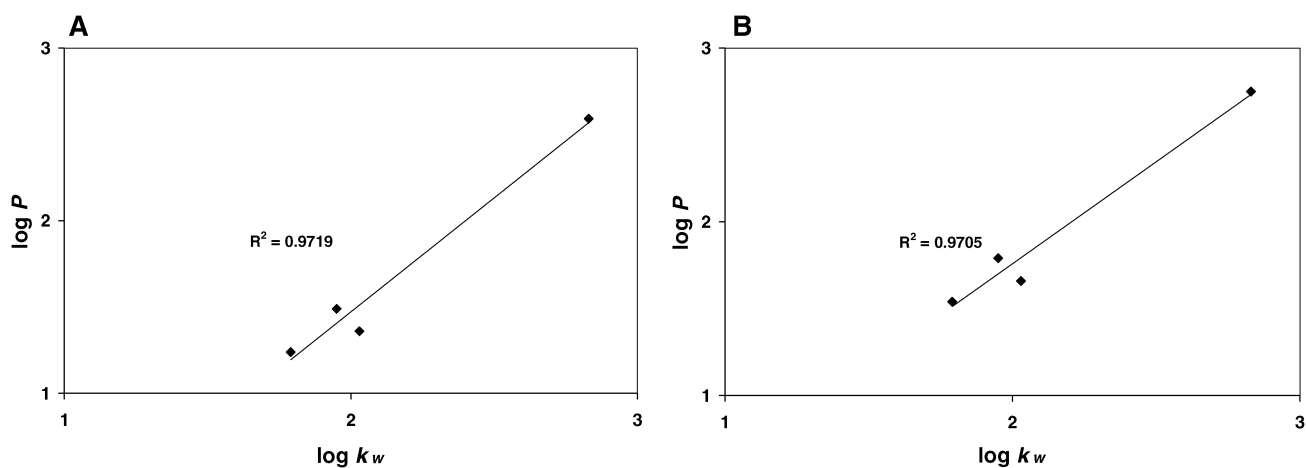
Fig. 2 Correlation between log k water (logarithm of capacity factor with 100% water as mobile phase extrapolated from the plot of log k vs. % acetonitrile for the four TSCs) and log P values obtained with ChemDraw Ultra 7.0 software (A) and log P values obtained with Spartan '02 software (B).

3.2 Thermal analysis

The ideal solubility of a solute is controlled by the melting point;[48] the thermal behaviour is a function of the solute–solute interactions in the crystalline lattice. The stronger these forces, the more insoluble the solute is. DSC data showed that TSCs display high T_m values (185–258 °C) that are consistent with strong solute–solute forces;[49] melting endotherms are unimodal. The introduction of one and two CH_3O– moieties increased the T_m pronouncedly from 185 °C to 229 °C and 258 °C, respectively. These results were in agreement with previous measurements[23] and could rely on both the increase of the molecular weight and the generation of stronger inter-molecular forces. Due to the additional molecular weight increase with respect to the non-allylated 5,6-dimethoxy derivative, an even higher T_m was expected for 5,6-dimethoxy-1-indanone N4-allylthiosemicarbazone. However, the T_m value decreased dramatically from 258 to 199 °C, probably due to the partial disruption of H bonds of terminal –NH_2 groups in the crystal lattice. Data suggest that the hydro-phobic domain in general and the methoxy substituents in particular play a key role in the consolidation of strong solute–solute associations of 1-indanone TSCs, these inter-actions being more crucial than the hydrophilic ones; 1-indanone TSC and 5,6-dimethoxy-1-indanone N4-allylthiosemicarbazone show similar T_m values. Since the solubilization process relies on the generation of strong solute–solvent attraction forces that overcome the solute–solute and solvent–solvent ones, the strong hydrophobic interactions found support the extremely low experimental aqueous solubility of these compounds (see below). These preliminary observations stress the relevance of characterizing comprehensively the solubilization and potential aggregation of TSCs in aqueous medium as a preamble to the biological evaluation. To the best of our knowledge, a study of this kind has not been conducted before.

3.3 Solubility of TSCs

The solubility of the different TSCs was investigated in pure DMSO and water–DMSO (98 : 2). The former is a good solvent for TSCs, while the latter is similar to the culture medium used in cell culture. Solutions of concentrations between 7.5 and 75 μM were prepared in both solvents and the UV absorption pattern monitored over time. This concentration range is in agreement with the well-established range of IC_{50} for most of the TSCs.[23,24,47] The UV absorption bands of the different TSCs are summarized in Table 1. The qualitative appearance of a new peak at 233 nm (239 nm for N4-allyl derivative) was observed for all the compounds exclusively in aqueous medium; the relative absorbance was stronger for higher TSC concentrations. This absorption peak did not comply with the Lambert-Beer law; this phenomenon was reported for other self-aggregating compounds.[39,40] Also, the absorbance ratio between the new peak and that at 312–330 nm ($I_{233}/I_{\lambda max}$) gradually increased over time (see below); the higher the T_m measured, the higher the relative intensity of this new peak. These data suggests the self-association of TSC molecules in water as previously depicted for amphotericin B and other drugs.[35,37,39]

To evaluate the physical stability of the solution, concentrations were monitored over 1 month. In DMSO, the solutions often showed relatively good stability, the intrinsic concentration of these TSCs being > 75 μM (Fig. 3). Having expressed this, 75 μM 5,6-dimethoxy-1-indanone showed a sharp, though not statistically significant, concentration loss at day 30. To confirm that TSCs are chemically stable in DMSO, solutions in 100% DMSO-d_6 were studied by ^{1}H-NMR. Only 2500 μM solutions could be analyzed reliably because of the low sensitivity of NMR equipment. Each drug candidate showed identical signals at days 0 and 90 and hydrolysis or oxidation was discarded.

When the physical stability was studied in water–DMSO, a different behaviour was observed. 1-indanone TSC showed high physical stability in the whole range of concentrations; S_o is 67.8 μM (Fig. 4). It is noticeable that the intensity of the peak at 233 nm was relatively weak ($I_{233}/I_{\lambda max}$ = 0.385 at day 30). Despite the lower lipophilicity predicted (and the higher aqueous solubility), 6-methoxy-1-indanone TSC was significantly less soluble (S_o = 31.1 μM). 7.5–37.5 μM solutions
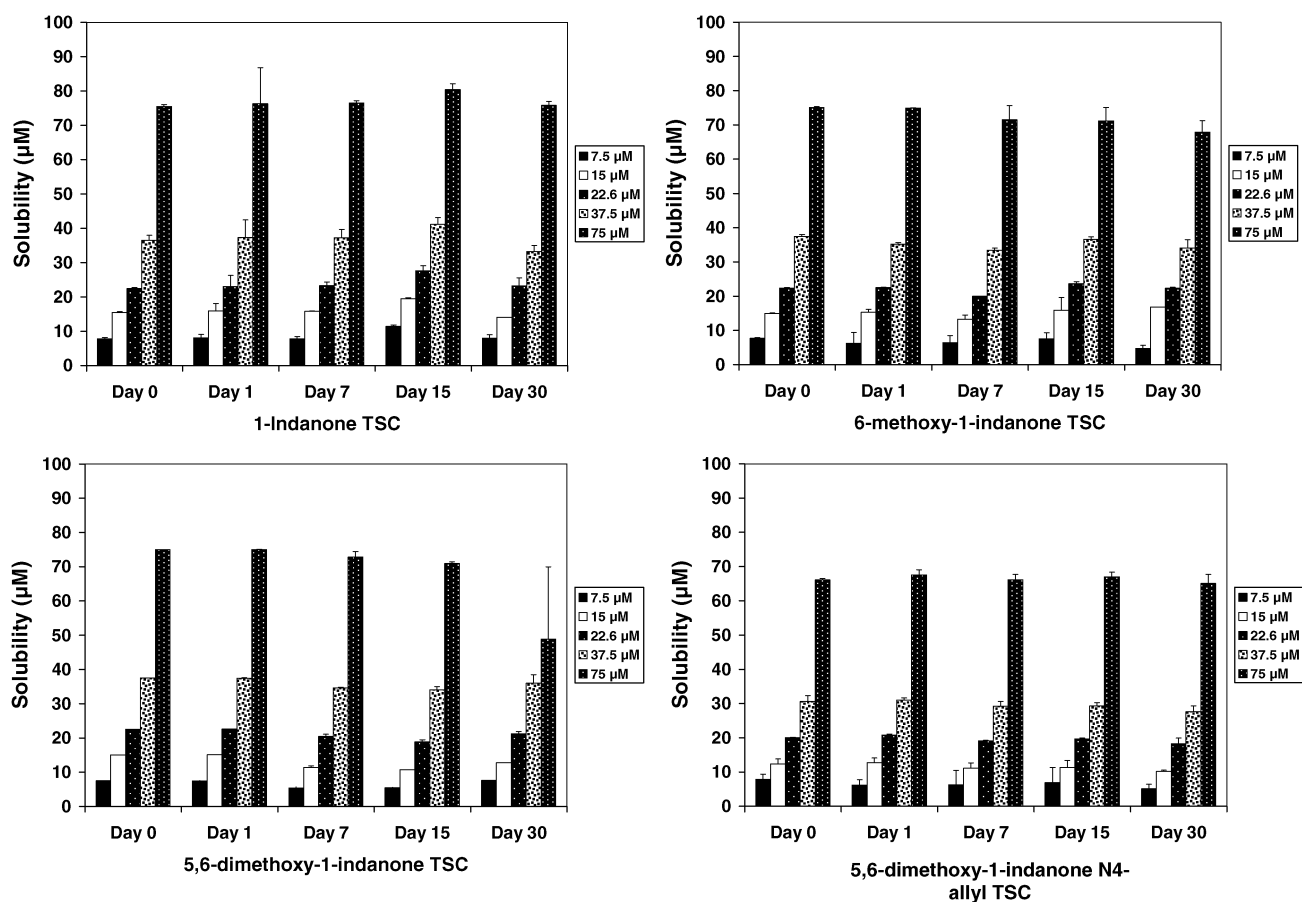
Fig. 3 Solubility of the different TSCs in DMSO, over 1 month.

remained unchanged, while a 75 μM sample showed a fast concentration loss even after 1 day. This phenomenon suggested the oversaturation of the system that resulted in a greater and a faster physical instability. Also, the aggregation peak showed a pronounced intensity increase ($I_{233}/I_{\lambda_{max}} = 0.654$ at day 30) with respect to 1-indanone TSC. 5,6-Dimethoxy-1-indanone TSC followed a similar trend though a substantially lower solubility ($S_o = 11.8$ μM) was found. In addition, $I_{233}/I_{\lambda_{max}}$ gradually increased from 0.450 at day 0, to 2.530 at day 15 and 4.630 at day 30 (Fig. S2, ESI†). According to all the theoretical and experimental data, 5,6-dimethoxy-1-indanone N4-allylthiosemicarbazone displays the highest lipophilicity of all the TSCs under investigation (Table 2). Thus, an even lower aqueous solubility was expected. However, data indicated that this TSC is more soluble ($S_o = 18.8$ μM) than the non-allylated counterpart. This behaviour was in agreement with the pronounced decrease in T_m. N-allylation disrupts, at least partially, the formation of H bonds and thus weakens both the solute–water and solute–solute interactions. It is remarkable that despite the relatively low theoretical and experimental lipophilicity, these TSCs display an extremely limited aqueous solubility. For example, the antiretroviral efavirenz (MW = 315.6749) presents a substantially higher lipophilicity than 5,6-dimethoxy-1-indanone TSC, the log P value being 5.4.[50] The intrinsic aqueous solubility of efavirenz is approximately 12.7 μM.[51] On the other hand, the T_m is substantially lower (138 °C).[52] Altogether, these results strongly

support that the strength of the solute–solute associations (and not the lipophilicity) is the main parameter governing the fast aggregation of TSCs in water; the hydrophobic interactions are probably more crucial than the hydrophilic ones as expressed by the less detrimental effect of allylation on solubility when compared to methoxylation.

3.4 Aggregation of TSCs

To characterize the self-aggregation pattern of 1-indanone TSCs, the size, intensity size distribution and zeta potential of TSC aqueous systems were measured over 1 month. It is remarkable that all the derivatives showed the instantaneous generation of one single population of nano-sized particles ranging between 120 and 300 nm (Fig. 5). The lower the S_o, the smaller the initial size measured; more particles of smaller size were probably generated. For example, 7.5 μM solutions of 1-indanone and 5,6-dimethoxy-1-indanone TSCs generated nanoparticles of 320 and 188 nm, respectively. The influence of the initial concentration is not clear though, often, the higher the concentration, the lower the initial size found. The spherical morphology of the aggregates was visualized by TEM as exemplified for 7.5 μM 5,6-dimethoxy-1-indanone TSC in Fig. 6A. At day 1, samples showed good stability as expressed by the almost unchanged sizes (Fig. 5). Having expressed this, some samples showed a sharp size increase without a clear trend. At later time points, a steady increase in the size
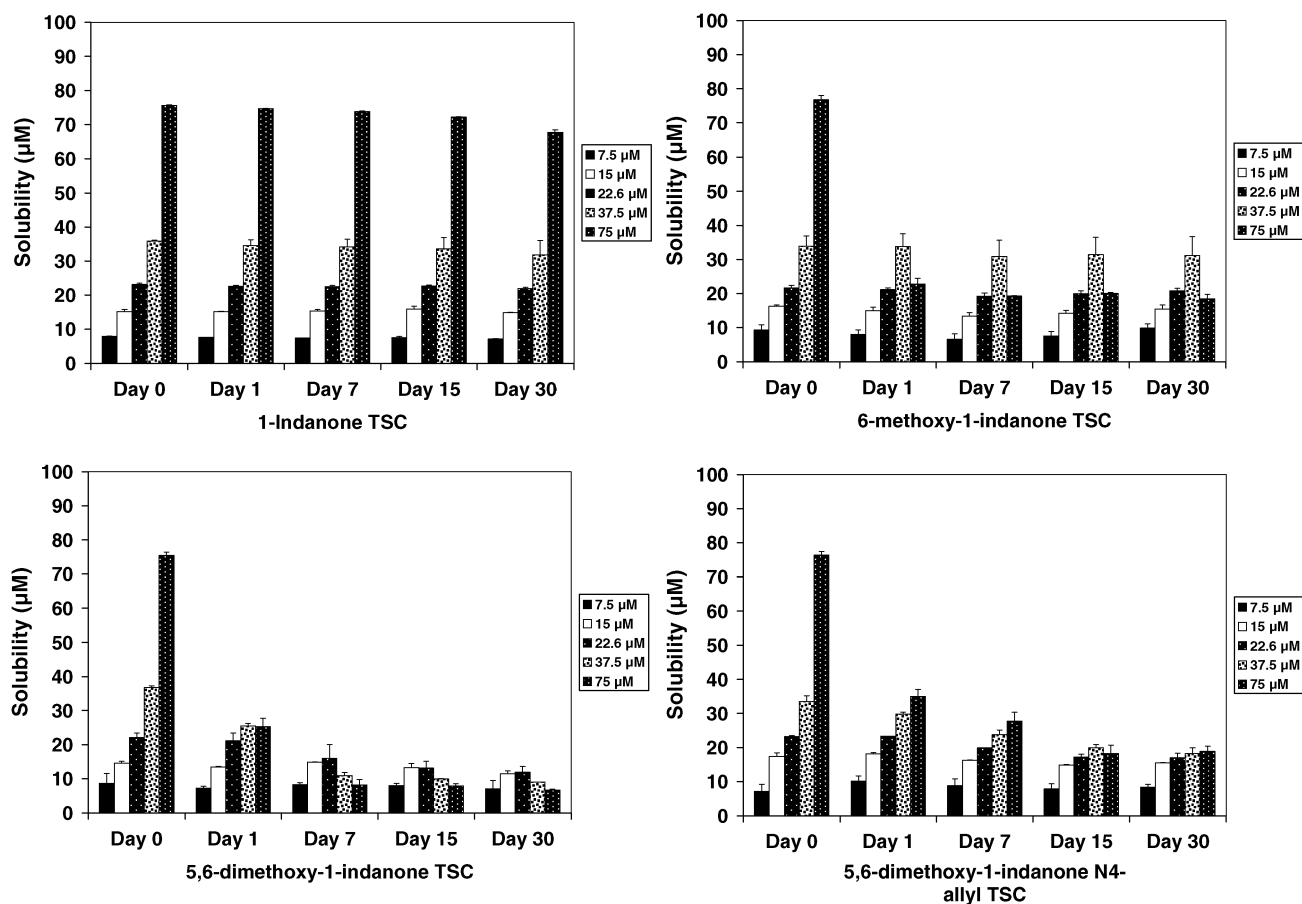
Fig. 4 Solubility of the different TSCs in water–DMSO (98 : 2), over 1 month.

of the structures was apparent; *e.g.*, 7.5 and 15.0 μM 5,6-dimethoxy-1-indanone TSC clusters grew from 162 and 184 nm at day 1 to 619 and 559 nm at day 7, respectively. It is worth stressing that these samples remained absolutely transparent to the naked eye and did not show significant absorbance (and concentration) changes during the same period of time (Fig. 4). These findings indicated that even when TSC concentrations seem to stay constant, the biological assays *in vitro* may be influenced by size changes; culture media is usually exchanged every 1–3 days. Thus, size changes within this time window are especially critical. In general, the size growth was accompanied by a sharp increase of the scattering intensity and the PDI that was consistent with the generation of broader size populations (Table 3). The scattering intensity percentage is roughly proportional to the concentration and sensitive to the formation of aggregates of larger size;[53] intensity values increased from 10–12% (day 0) to 25–45% (day 30). This phenomenon was presumably related to the uncontrolled super-aggregation of the initially formed nanoparticles. Consequently, aggregates with sizes of 550 nm and up to 1 μm were observed at day 30. These results suggest that the initial nanoparticles serve as nucleation sites for the later deposition of more TSC molecules. This mechanism is strongly supported by the appearance of micron-sized clusters in TEM analysis at day 30 that would be in agreement with the presence of amorphous crystals (Fig. 6B). Also, some small spherical aggregates were still visualized (Fig. 6B, inset). When

highly concentrated solutions (150 μM) were prepared in water–DMSO (98 : 2), TSCs precipitated instantaneously forming well-defined rhomboid crystals, as shown for 5,6-dimethoxy-1-indanone TSC in Fig. 6C. These results together with DSC analysis strongly suggest that the initial structures correspond to amorphous nano-crystals that gradually grow in size over time (Fig. 6B). This behaviour is in full agreement with a previous study investigating the aggregation of non-nucleoside reverse transcriptase inhibitors by DLS[38] and, as shown also in the present work, it is concentration-dependent.

Zeta potential is a measure of the charge density on the surface of the particles and depends on (i) the concentration of the charged moieties and (ii) the size of the particle.[54] A key factor that may affect zeta potential is pH; TSC solutions in water–DMSO displayed pH-values between 6 and 7. Data clearly indicated the negatively-charged surface of all the TSCs, the values ranging from −8.68 mV down to −16.53 mV at day 0 (Table 4). In general, these values were not sufficiently negative to stabilize the colloidal system by repulsion.[55] 5,6-Dimethoxy-1-indanone TSC solubilized in 100% ultra-pure water also showed negative values (approximately −10 mV). The electronegative nature of the surface could be associated with the fact that the C=S group is available in its thiolato anionic form. This hypothesis is supported by the relatively acid character of the –NH– moiety of –C=N–*NH*–C(=S)–NH$_2$[56] that enables the coordination of the TSC molecule either as neutral or anionic ligand.[57] When
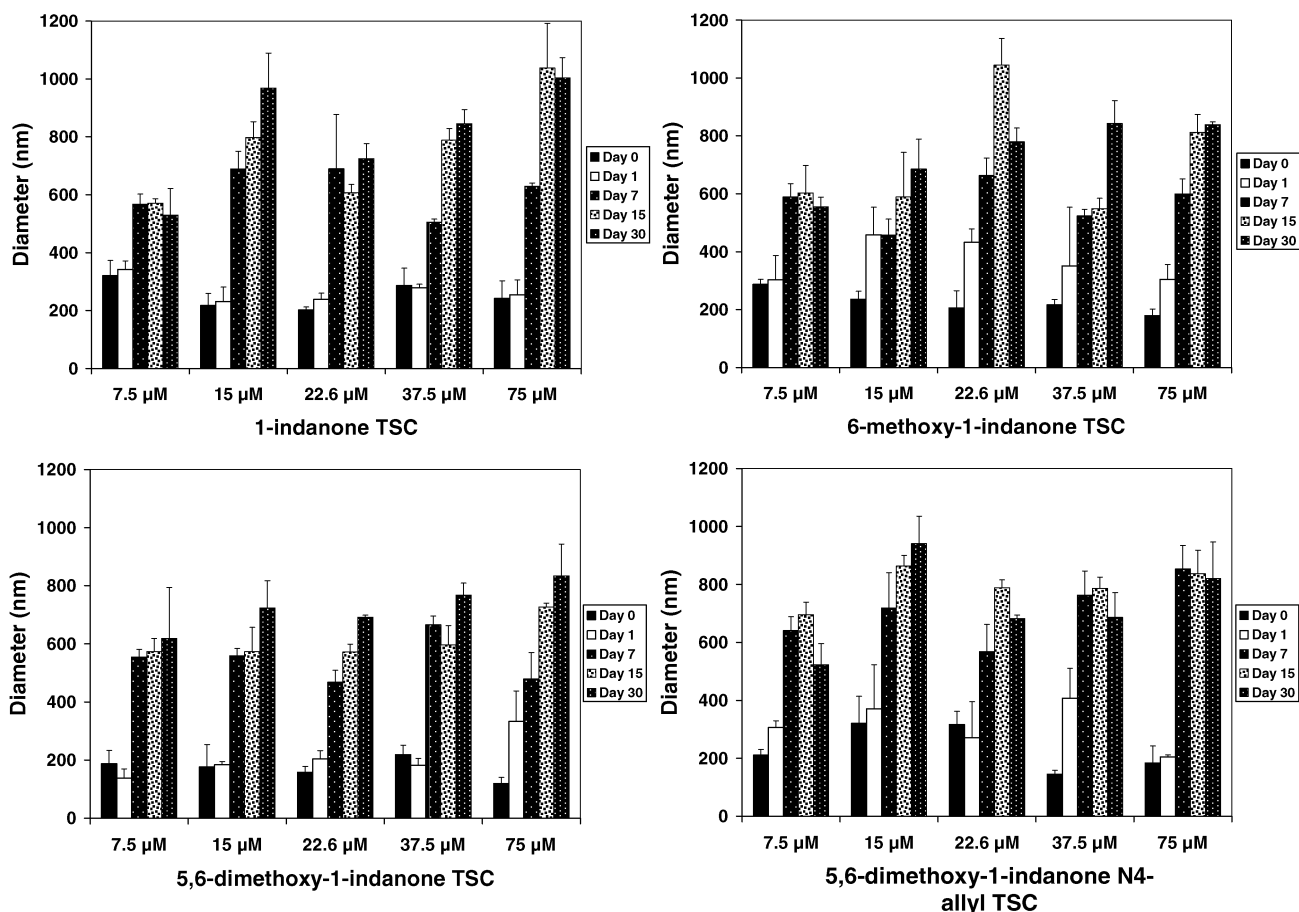
Fig. 5 Hydrodynamic diameter of TSC aggregates generated in water–DMSO (98 : 2) measured by DLS, over 1 month.

coordinated as anionic ligand, the unsaturated conjugated system is extended to include the sulfur atom and forms a negatively-charged C=N–N=C(–S$^{(-)}$)–N– group. It has been proposed that this conjugation system enhances the biological activity of these compounds.[58] High-resolution X-ray diffraction experiments currently ongoing support this hypothesis (data not shown). These findings would suggest that the interaction of highly hydrophobic aromatic rings of TSCs is the primary arrangement. This would lead to the generation of an inner hydrophobic "core" that is surface-decorated by negatively-charged hydrophilic chains belonging to the thiosemicarbazone residue. The explanation that the aggregation process is initiated by the strong interaction between the hydrophobic portions of the molecule is supported by the fact that methoxylation of the aromatic ring dramatically strengthens the solute–solute affinity, as expressed by the sharp increase in T_m and makes these derivatives much more water-insoluble. In general, the larger the particle, the less negative the zeta potential (for similar charge concentrations on the surface) found.[53] Despite the size growth found in our experiments, zeta potential values tended to be more negative at later time points. These findings would suggest some electronic rearrangement over time; an increasing number of negatively-charged groups are gradually being exposed at the surface. Having said this, further studies are demanded to confirm this hypothesis.

3.5 Surface tension

Previous works reported that the self-aggregation of relatively large amphiphilic drug molecules leads to the formation of micelles.[32–36] Micellar systems are characterized by the minimum concentration required for the formation of micelles at a given temperature, namely the critical micellar concentration (CMC). A measurable phenomenon associated with micellization is the sharp decrease of the surface tension of the solvent at the given CMC. As depicted above, 1-indanone TSCs present two well defined regions, the hydrophobic aromatic ring and the hydrophilic thiosemicarbazide portion (Table 1). Aiming to elucidate whether the aggregates display a micelle-like behaviour, the surface tension was measured for TSC solutions ranging between 0 and 75 µM. However, no changes were found with respect to the pure solvent, indicating that TSCs do not generate micellar systems (not shown).

4. Summary

The present work thoroughly investigated the aggregation performance of potentially antiviral 1-indanone TSCs; this study constitutes the first report of its kind. Regardless of the relatively low lipophilicity predicted by theoretical calculations, these compounds are very insoluble in water. This performance is especially notorious for methoxylated (and non-N-allylated)
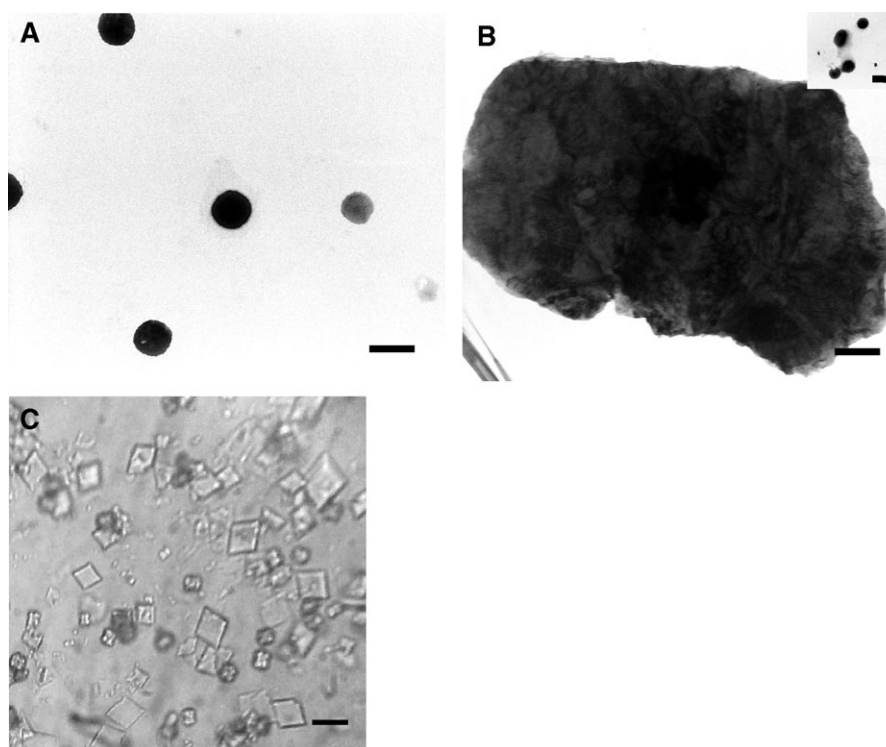
Fig. 6 (A,B) TEM micrographs of 7.5 μM 5,6,-dimethoxy-1-indanone TSC aggregates in water–DMSO (98 : 2) stained with 2% phosphotungstic acid. (A) day 0 and (B) day 30. Scale bar = 100 nm. (C) Optical microscope micrograph of 150 μM 5,6-dimethoxy-1-indanone TSC aggregates in water–DMSO (98 : 2) at day 0. Scale bar = 10 μm.

Table 3 Polydispersity (PDI) data of TSC nanoparticles over 1 month, as measured by DLS

		Polydispersity (PDI) (±SD)				
		Time (days)				
TSC	Concentration/μM	0	1	7	15	30
1-Indanone thiosemicarbazone	7.5	0.382 (0.090)	0.430 (0.015)	0.633 (0.036)	0.714 (0.041)	0.681 (0.054)
	15	0.325 (0.060)	0.402 (0.127)	0.588 (0.141)	0.715 (0.182)	0.606 (0.016)
	22.6	0.323 (0.052)	0.350 (0.036)	0.493 (0.125)	0.531 (0.031)	0.535 (0.042)
	37.5	0.444 (0.086)	0.464 (0.129)	0.674 (0.040)	0.576 (0.068)	0.591 (0.050)
	75	0.343 (0.048)	0.362 (0.032)	0.605 (0.131)	0.638 (0.103)	0.497 (0.058)
6-methoxy-1-indanone thiosemicarbazone	7.5	0.302 (0.028)	0.701 (0.077)	0.472 (0.074)	0.539 (0.039)	0.625 (0.015)
	15	0.479 (0.040)	0.703 (0.108)	0.557 (0.096)	0.470 (0.042)	0.596 (0.064)
	22.6	0.428 (0.157)	0.611 (0.152)	0.486 (0.033)	0.522 (0.098)	0.445 (0.117)
	37.5	0.402 (0.077)	0.581 (0.045)	0.606 (0.053)	0.677 (0.049)	0.333 (0.195)
	75	0.358 (0.103)	0.672 (0.098)	0.525 (0.061)	0.695 (0.033)	0.492 (0.025)
5,6-dimethoxy-1-indanone thiosemicarbazone	7.5	0.350 (0.017)	0.189 (0.039)	0.433 (0.031)	0.631 (0.048)	0.617 (0.041)
	15	0.410 (0.094)	0.371 (0.078)	0.572 (0.061)	0.465 (0.030)	0.548 (0.094)
	22.6	0.444 (0.021)	0.387 (0.052)	0.492 (0.099)	0.585 (0.013)	0.673 (0.052)
	37.5	0.387 (0.051)	0.325 (0.046)	0.560 (0.019)	0.630 (0.042)	0.508 (0.024)
	75	0.505 (0.491)	0.462 (0.024)	0.647 (0.007)	0.461 (0.257)	0.644 (0.077)
5,6-dimethoxy-1-indanone N4-allyl thiosemicarbazone	7.5	0.367 (0.130)	0.734 (0.171)	0.649 (0.143)	0.386 (0.049)	0.370 (0.030)
	15	0.426 (0.085)	0.837 (0.152)	0.589 (0.022)	0.475 (0.019)	0.337 (0.037)
	22.6	0.433 (0.107)	0.756 (0.078)	0.546 (0.092)	0.398 (0.050)	0.337 (0.037)
	37.5	0.369 (0.076)	0.477 (0.069)	0.536 (0.128)	0.313 (0.187)	0.514 (0.033)
	75	0.458 (0.145)	0.312 (0.051)	0.608 (0.038)	0.640 (0.077)	0.705 (0.047)

derivatives. The formation of nano-aggregates in water was revealed by the appearance of a new strong absorption peak at 233–239 nm in the UV. DLS analysis showed that the initially nanoscopic particles (120–300 nm) gradually grew to generate larger structures that remained invisible. Results of biological assays *in vitro* under these conditions could be seriously misleading, as compounds are not really dissolved in the

culture medium. This phenomenon is even more dramatic when TSC stock aqueous solutions are prepared and used over several weeks assuming that the solutions remain unaltered.

Overall findings point out the strength of the solute–solute interaction as the main parameter that rules the solubilization process and stress the relevance of characterizing thoroughly the solubility and the aggregation of these novel drug candidates in

Table 4 Zeta potential values of the different 1-indanone TSCs over 1 month

| TSC | Concentration/μM | Zeta potential (±SD)/mV | | | | |
| | | Time (days) | | | | |
		0	1	7	15	30
1-indanone thiosemicarbazone	7.5	−16.53 (2.77)	−16.00 (2.12)	−7.50 (2.80)	−11.21 (2.81)	−16.65 (3.61)
	15	−17.03 (3.19)	−14.05 (2.76)	−7.24 (0.33)	−16.55 (0.21)	−19.00 (2.83)
	22.6	−12.57 (4.10)	−14.50 (3.39)	−5.66 (0.48)	−11.40 (0.57)	−12.80 (0.99)
	37.5	−15.40 (0.28)	−15.30 (7.07)	−11.32 (5.0)	−13.75 (0.07)	−20.65 (0.49)
	75	−12.36 (9.67)	−11.00 (1.41)	−15.10 (0.20)	−15.03 (1.81)	−16.97 (3.02)
6-methoxy-1-indanone thiosemicarbazone	7.5	−8.68 (1.53)	−10.35 (0.21)	−10.70 (0.71)	−14.35 (0.49)	−13.85 (0.07)
	15	−11.76 (4.73)	−15.50 (1.70)	−8.25 (0.35)	−15.35 (1.06)	−17.15 (0.21)
	22.6	−7.75 (0.18)	−13.55 (3.32)	−6.84 (0.44)	−7.67 (0.81)	−15.25 (0.07)
	37.5	−11.85 (1.20)	−9.51 (1.12)	−9.12 (0.71)	−12.25 (0.35)	−14.80 (0.28)
	75	−11.90 (2.55)	−7.17 (0.01)	−13.37 (0.65)	−9.15 (0.51)	−12.10 (2.43)
5,6-dimethoxy-1-indanone thiosemicarbazone	7.5	−15.13 (4.90)	−24.55 (3.32)	−19.95 (5.02)	−20.35 (7.99)	−10.53 (0.64)
	15	−23.95 (4.45)	−21.95 (6.58)	−19.43 (3.29)	−12.55 (2.47)	−6.29 (1.58)
	22.6	−12.57 (1.20)	−20.75 (2.47)	−10.48 (0.31)	−28.97 (2.89)	−11.70 (0.57)
	37.5	−4.21 (1.61)	−24.90 (1.61)	−16.67 (1.07)	−19.70 (3.65)	−12.10 (2.55)
	75	−9.47 (2.71)	−9.33 (3.25)	−18.07 (1.62)	−19.67 (3.59)	−16.58 (1.65)
5,6-dimethoxy-1-indanone N4-allyl thiosemicarbazone	7.5	−12.10 (2.83)	−9.35 (0.69)	−12.35 (1.48)	−12.50 (1.13)	−15.30 (3.39)
	15	−10.79 (2.14)	−11.05 (0.64)	−11.65 (0.35)	−11.05 (0.21)	−12.40 (0.85)
	22.6	−5.64 (2.51)	−11.65 (0.35)	−11.85 (0.35)	−12.25 (0.07)	−12.35 (0.64)
	37.5	−5.74 (0.04)	−9.20 (0.11)	−9.09 (0.01)	−9.35 (1.07)	−10.60 (0.28)
	75	−9.94 (4.33)	−7.57 (4.72)	−16.87 (3.23)	−23.80 (1.74)	−19.33 (1.96)

aqueous media before one proceeds to any biological evaluation. For these compounds, solubility predictions based on theoretical or experimental lipophilicity calculations are not reliable. Current investigations are being dedicated to gain further insight into the crystallization process, the aggregation pattern of these TSCs in culture medium and their potential stabilization by means of different nanotechnology approaches.

References

1 G. Domagk, *Irish J. Med. Sci.*, 1951, **26**, 474–485.
2 H. H. Vollhaber, *Therapiewoche*, 1983, **33**, 5345–5351.
3 Z. Iakovidou, A. Papageorgiou, M. A. Demertzis, E. Mioglou, D. Mourelatos, A. Kotsis, P. Nath Yadav and D. Kovala-Demertzi, *Anti-Cancer Drugs*, 2001, **12**, 65–70.
4 D. Sriram, P. Yogeeswari, P. Dhakla, P. Senthilkumar and D. Banerjee, *Bioorg. Med. Chem. Lett.*, 2007, **17**, 1888–1891.
5 A. K. Halve, B. Bhashkar, V. Sharma, R. Bhadauria, A. Kankoriya, A. Soni and K. Tiwari, *J. Enzyme Inhib. Med. Chem.*, 2008, **23**, 77–81.
6 X. Du, C. Guo, E. Hansell, P. S. Doyle, C. R. Caffrey, T. P. Holler, J. H. McKerrow and F. E. Cohen, *J. Med. Chem.*, 2002, **45**, 2695–2707.
7 I. C. Mendes, L. R. Teixeira, R. Lima, H. Beraldo, N. L. Speziali and D. X. West, *J. Mol. Struct.*, 2001, **559**, 355–360.
8 V. Mishra, S. N. Pandeya, C. Pannecouque, M. Witvrouw and E. De Clercq, *Arch. Pharm.*, 2002, **335**, 183–186.
9 T. R. Bal, B. Anand, P. Yogeeswari and D. Sriram, *Bioorg. Med. Chem. Lett.*, 2005, **15**, 4451–4455.
10 R. P. Bhamaria, R. A. Bellare and C. V. Deliwala, *Indian J. Exp. Biol.*, 1968, **6**, 62–63.
11 A. B. Tadros and M. El-Batouti, *Anti-Corros. Methods Mater.*, 2004, **51**, 406–413.

12 S. S. Konstantinovic, B. C. Radovanovic, S. P. Sovilj and S. Stanojevic, *J. Serb. Chem. Soc.*, 2008, **73**, 7–13.

13 N. Birch and X. Wang H.-S. Chong, *Expert Opin. Ther. Pat.*, 2006, **16**, 1533–1556.

14 I. K. M. Morton and J. M. Hall, in: *Concise dictionary of pharmacological agents: Properties and synonyms*, Kluwer Academic Publishers, Dordrecht, The Netherlands, 1999.

15 M. C. Pirrung, S. V. Pansare, K. D. Sarma, K. A. Keith and E. R. Kern, *J. Med. Chem.*, 2005, **48**, 3045–3050.

16 R. A. Finch, M.-C. Liu, S. P. Grill, W. C. Rose, R. Loomis, K. M. Vasquez, Y.-C. Cheng and A. C. Sartorelli, *Biochem. Pharmacol.*, 2000, **59**, 983–991.

17 Y. Yu, D. S. Kalinowski, Z. Kovacevic, A. R. Siafakas, P. J. Jansson, C. Stefani, D. B. Lovejoy, P. C. Sharpe, P. V. Bernhardt and D. R. Richardson, *J. Med. Chem.*, 2009, **52**, 5271–5294.

18 M.-X. Li, C.-L. Chen, C.-S. Ling, J. Zhou, B.-S. Ji, Y.-J. Wu and J.-Y. Niu, *Bioorg. Med. Chem. Lett.*, 2009, **19**, 2704–2706.

19 B. N. Brousse, A. G. Moglioni, M. Martins Alho, A. Álvarez-Larena, G. Y. Moltrasio and N. B. D'Accorso, *ARKIVOC*, 2002, (x), 14–23.

20 P. D. Rouge, B. N. Brousse, A. G. Moglioni, G. A. Cozzi, A. Alvarez-Larena, N. D'Accorso and G. Y. Moltrasio, *ARKIVOC*, 2005, (xii), 8–21.

21 B. N. Brousse, R. Massa, A. G. Moglioni, M. Martins Alho, N. D'Accorso, G. Gutkind and G. Y. Moltrasio, *J. Chil. Chem. Soc.*, 2004, **49**, 45–49.

22 C. Garcia, B. Brousse, M. Carlucci, A. Moglioni, M. Martins Alho, G. Moltrasio, N. D'Accorso and E. B. Damonte, *Antiviral Chem. Chemother.*, 2003, **14**, 99–105.

23 L. M. Finkielsztein, E. F. Castro, L. E. Fabián, G. Y. Moltrasio, R. H. Campos, L. V. Cavallaro and A. G. Moglioni, *Eur. J. Med. Chem.*, 2008, **43**, 1767–73.

24 D. Durantel, N. Branza-Nichita, S. Durantel, R. A. Dweek and N. Zitzmann, *Adv. Exp. Med. Biol.*, 2005, **564**, 5–6.

25 A. S. Qureshi, H. Qureshi and A. Hameed, *Eur. J. Clin. Microbiol. Infect. Dis.*, 2009, **28**, 1409–1413.

26 A. G. Moglioni, unpublished results.

27 B. Christenson, J. R. Rodríguez, H. F. Gorbea and C. H. Ramírez-Ronda, *Antimicrob. Agents Chemother.*, 1985, **27**, 570–573.

28 A. S. Dobek, D. L. Klayman, E. T. Dickson Jr., J. P. Scovill and E. C. Tramont, *Antimicrob. Agents Chemother.*, 1980, **18**, 27–36.

29 M. D. Hall, N. K. Salam, J. L. Hellawell, H. M. Fales, C. B. Kensler, J. A. Ludwig, G. Szakacs, D. E. Hibbs and M. M. Gottesman, *J. Med. Chem.*, 2009, **52**, 3191–3204.

30 C. A. Lipinski, F. Lombardo, B. W. Dominy and P. J. Feeney, *Adv. Drug Delivery Rev.*, 2001, **46**, 3–26.

31 T. Fujita, J. Iwasa and C. Hansch, *J. Am. Chem. Soc.*, 1964, **86**, 5175–5180.

32 P. Taboada, D. Attwood, J. M. Ruso, F. Sarmiento and V. Mosquera, *Langmuir*, 1999, **15**, 2022–2028.

33 P. Taboada, D. Attwood, M. Garcia, M. N. Jones, J. M. Ruso, V. Mosquera and F. Sarmiento, *J. Colloid Interface Sci.*, 2000, **221**, 242–245.

34 D. Attwood, E. Boitard, J.-P. Dubes and H. Tachoire, *J. Colloid Interface Sci.*, 2000, **227**, 356–362.

35 M. A. Cheema, M. Siddiq, S. Barbosa, P. Taboada and V. Mosquera, *J. Chem. Eng. Data*, 2008, **53**, 368–373.

36 Z. Shervani, H. Etori, K. Taga, T. Yoshida and H. Okabayashi, *Colloids Surf., B*, 1996, **7**, 31–38.

37 R. Espada, S. Valdespina, C. Alfonso, G. Rivas, M. P. Ballesteros and J. J. Torrado, *Int. J. Pharm.*, 2008, **361**, 64–69.

38 Y. Volovik Frenkel, A. D. Clark, K. Das, Y.-H. Wang, P. J. Lewi, P. A. J. Janssen and E. Arnold, *J. Med. Chem.*, 2005, **48**, 1974–1983.

39 J. M. López-Nicolás and F. García-Carmona, *Food Chem.*, 2010, **118**, 648–655.

40 D. A. Fernandez, J. Awruch and L. E. Dicelio, *J. Photochem. Photobiol., B*, 1997, **41**, 227–232.

41 C. Hansch and A. Leo, *Substituent Constants for Correlation Analysis in Chemistry and Biology*, Wiley-Interscience, New York, 1979.

42 *A physical chemical basis for the design of orally active prodrugs*, in *Drug Design*, ed. S. H. Yalkowsky, W. Morozowich and E. J. Ariens, Academic Press, New York, 1980, vol. 9.

43 M.-M. Hsieh and J. O. Dorsey, *Anal. Chem.*, 1995, **67**, 48–57.

44 D. Casoni, A. Kot-Wasik, J. Namiénisk and C. Sârbu, *J. Chromatogr., A*, 2009, **1216**, 2456–2465.

45 Z. Mrkvičkov, P. Kovařkov, S. Balíková and J. Klimeš, *J. Pharm. Biomed. Anal.*, 2008, **48**, 310–314.

46 H. Beraldo, *Quim. Nova*, 2004, **27**, 461–471.

47 I. Đilović, M. Rubčić, V. Vrdoljak, S. Kraljević Pavelić, M. Kralj, I. Piantanida and M. Cindrić, *Bioorg. Med. Chem.*, 2008, **16**, 5189–5198.

48 F. Martínez, C. M. Ávila and A. Gómez, *J. Braz. Chem. Soc.*, 2003, **14**, 803–808.

49 D. A. Chiappetta, J. Degrossi, R. A. Lizarazo, D. L. Salinas, F. Martínez and A. Sosnik, in *Polymer aging, stabilizers and amphiphilic block copolymers*, ed. L. Segewicz and M. Petrowsky, Nova Science Publishers, Hauppauge, NY, 2010, pp. 197–211.

50 R. Tanaka, E. Hanabusa, E. Kinai, N. Hasegawa, M. Negishi and S. Kato, *Antimicrob. Agents Chemother.*, 2008, **52**, 782–785.

51 D. A. Chiappetta, C. Hocht, C. Taira and A. Sosnik, *Nanomedicine*, 2010, **5**, 11–23.

52 D. A. Chiappetta, C. Hocht and A. Sosnik, *Curr. HIV Res.*, 2010, **8**, 223–231.

53 D. Shaw and P. Dubin, Application note MRK505-01, Malvern Instruments.

54 Y. Chen, G. Cui, M. Zhao, C. Wang, K. Qian, S. Morris-Natschke, K.-H. Lee and S. Peng, *Bioorg. Med. Chem.*, 2008, **16**, 5914–5925.

55 T. M. Riddick, *Zeta-Meter Manual*, Zeta Meter Inc., 1968.

56 D. R. Richardson, P. C. Sharpe, D. B. Lovejoy, D. Senaratne, D. S. Kalinowski, M. Islam and P. V. Bernhardt, *J. Med. Chem.*, 2006, **49**, 6510–6521.

57 E. Bermejo, A. Castiñeiras, I. García and D. X. West, *Polyhedron*, 2003, **22**, 1147–1154.

58 L. Latheef, E. B. Seena and M. R. P. Kurup, *Inorg. Chim. Acta*, 2009, **362**, 2515–2518.